Proceedings of the 16th European VLBI Network Symposium
Ros, E., Benke, P., Dzib, S., Rottmann, I., & Zensus, J.A. (eds.)
September 2nd-6th 2024, Bonn, Germany

Polarization flare of 3C 454.3 in millimeter wavelengths seen from decadal polarimetric monitoring data sets

H.-W. Jeong[1,2], S.-S. Lee[1,2,⋆], S. Kang[2], M. Kam[3,4], S. Kim[1,2], W. Y. Cheong[1,2], D.-Y. Byun[1,2], C. Song[1,2], and S. Trippe[4,5]

[1] Astronomy and Space Science, University of Science and Technology, 217 Gajeong-ro, Yuseong-gu, Daejeon 34113, Republic of Korea
[2] Korea Astronomy and Space Science Institute, 776 Daedeok-daero, Yuseong-gu, Daejeon 34055, Republic of Korea
[3] Institute of Astronomy and Astrophysics, Academia Sinica, P.O. Box 23-141, Taipei 10617, Taiwan
[4] Department of Physics and Astronomy, Seoul National University, Gwanak-gu, Seoul 08826, Republic of Korea
[5] SNU Astronomy Research Center, Seoul National University, Gwanak-gu, Seoul 08826, Korea

Abstract. This study investigates polarimetric characteristics of the blazar 3C 454.3 ($z = 0.859$) at 22–129 GHz using decadal (2011–2022) data sets. The corresponding data sets were obtained from the single-dish (SD) mode observations of the Korean VLBI Network (KVN) and the 43-GHz Very Long Baseline Array (VLBA). We found that the linear polarization angle is preferred to be $\sim 100^\circ$ when the source is highly polarized. Polarized flux density from the KVN SD and VLBA at 43 GHz is comparable (i.e., $\Delta S_\mathrm{p}/S_\mathrm{p} \approx 2\%$), and the polarization angles display similar rotation, indicating a negligible convolution effect from an extended jet beyond the scale of VLBA 43 GHz. We found an interesting, notable polarization flare (PF) in the KVN SD data in 2019 in the frequency range of 22–129 GHz. During the flare, the observed polarization angles rotate from $\sim 150^\circ$ to $\sim 100^\circ$ at all frequencies with chromatic polarization degree. Based on the observed polarization properties, we suggest that PF in 2019 is attributed to the shock–shock interaction in the stationary region. Change in the viewing angle of the jet alone is insufficient to describe the increase in brightness temperature, indicating the presence of source intrinsic processes, such as, e.g., particle acceleration.

1. Introduction

The blazar is a subclass of Active Galactic Nucleus (AGN), in which a relativistic jet is inclined with a small viewing angle between the jet and the line-of-sight. The small viewing angle of the jet enhances the Doppler boosting effects, leading to rapid variability. The jet emits radiation over the entire range of electromagnetic waves, which is dominated by synchrotron radiation from radio to optical bands, and radiation by inverse-Compton scattering in higher energy bands (e.g., γ-ray). Synchrotron radiation is emitted by relativistic electrons gyrating around magnetic field lines in the jet and is most likely polarized, with its polarized properties strongly constrained by magnetic field environments in the jet. If the field lines in the jets are well-ordered and strong, one may observe a high degree of linear polarization (m_p) and high polarized flux density (S_p). Observational results have identified polarized emission from AGN. Both m_p and the polarization angle (χ) offer information about the magnetic field lines.

2. Observations

MOGABA (MOnitoring of GAmma-ray Bright Active galactic nuclei; Kang et al., 2015) is one of the polarimetric monitoring programs using the KVN on AGNs through SD mode. Another monitoring program, PAGaN (Plasma-physics of Active Galactic Nuclei; Park et al., 2018), also has been conducted for VLBI polarimetry, and their joint SD observation is used to calibrate the absolute polarization angle (Kam et al., 2023). 3C 454.3 is one of the target sources of MOGABA and PAGaN. This work used polarimetric monitoring data in the time periods 2011–2022 (MOGABA) and 2016–2022 (PAGaN) from the KVN 21-m radio telescopes at 22, 43, 86, and 129 GHz on 3C 454.3 in SD mode (Jeong et al., in prep.). The polarimetric observables are recorded via the circularly polarized feed horns in the KVN receiver.

We also employed high angular resolution VLBA observations at 43 GHz from VLBA-BU-BLAZAR (Jorstad et al., 2017; Weaver et al., 2022) in the period from January 2011 to June 2022. Thanks to the long baseline length of the VLBA, 3C 454.3 has been resolved into a compact radio core at the end of the east side with an extended jet structure in the northeastern direction. We used the CLEAN algorithm (e.g., Högbom, 1974; Clark, 1980; Cornwell et al., 1999) for imaging and `modelfit` task with circular Gaussian models in the `DIFMAP` software (Shepherd, 1997) to measure the respective locations of the radio core and Region C.

⋆ Corresponding author. e-mail: sslee@kasi.re.kr

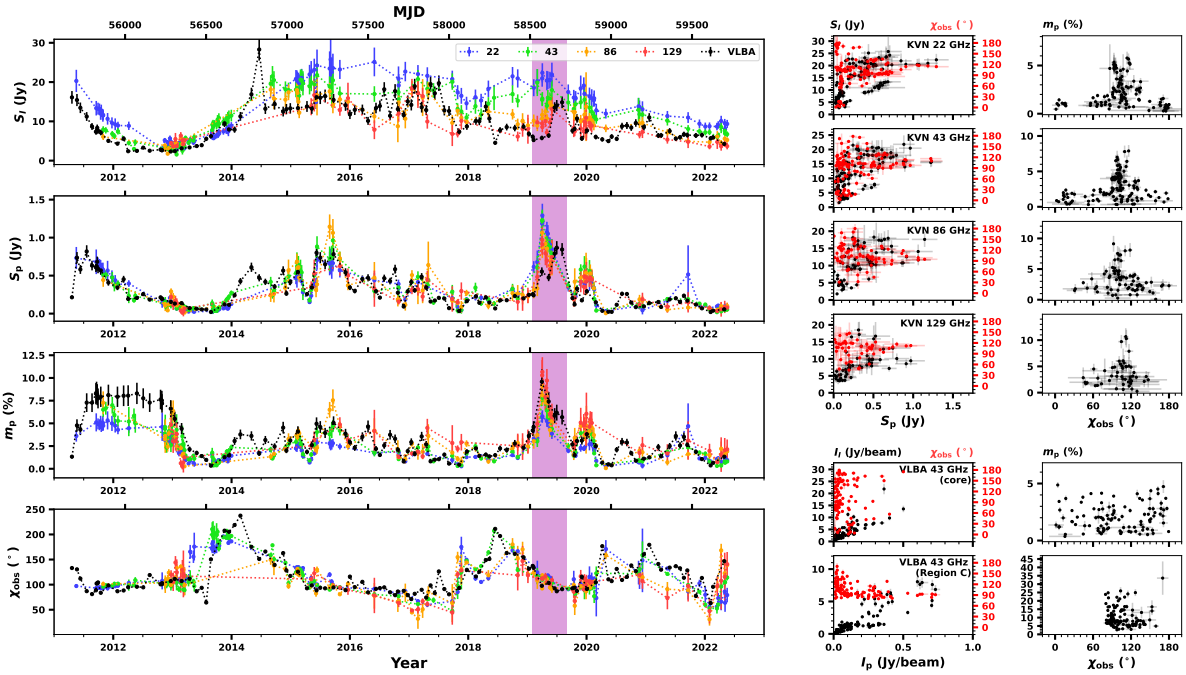

Fig. 1. Left: from top to bottom, each panel shows total flux density (S_I), polarized flux density (S_p), polarization degree (m_p), and polarization angle (χ_obs). Right: correlation of the measurements from the KVN in the first four rows and VLBA 43 GHz in the last two rows. The VLBA data in the correlation plots are obtained by averaging pixels on where the core and Region C are located based on the Gaussian models (Jeong et al., in prep.).

3. Results and Conclusions

Figure 1 shows the light curves in the left panel and correlations of polarimetric measurements in the right panel. At 43 GHz, we have compared measurements from the KVN SD and VLBA and found consistent polarized emission (a difference of $2 \pm 7\%$ within a week) in scales of arcsecond and mas. In addition, polarization angles are also comparable to each other, indicating a negligible effect from extended jet structure beyond a few mas scale. As shown in the right panels in Figure 1, polarization angle (χ_obs) appears near 100° when the source is strongly polarized, observed between 22 and 129 GHz. This characteristic also appears from Region C, which is a downstream jet region about 0.6 mas from the core.

In 2019, even though the increase in total flux density (S_I) is not prominent, its polarized flux density (S_p) is strongly enhanced with a maximum m_p of about 10%. At the same time, χ_obs was being aligned parallel with the jet direction ($\sim -80°$, Weaver et al., 2022). The increasing factor in S_p is about an order at 22 GHz, being a polarization flare (PF). Given the large beam sizes of the KVN SD, we are restricted to investigating the location and origin of the PF. Meanwhile, the high-resolution maps from the 43-GHz VLBA observations show an increase in polarized emission in Region C when a moving knot[1] arrived as shown in Figure 2. In addition, while the polarized emission in Region C is strong, it is weak in the core, indicating Region C is the origin of PF rather than the core. Moreover, as shown in Figure 1, the consistent evolution for PF among the observing frequencies also supports Region C as the origin of PF.

Although the observed polarization angle χ_obs most likely provides us with information about the orientation of magnetic field lines in the jet, the Faraday effect contaminates the intrinsic polarized emission when the emission propagates through an ionized medium with magnetic field lines (Burn, 1966; Sokoloff et al., 1998). This leads to a rotation of χ, which is proportional to the squared wavelength, i.e., $\Delta\chi \propto \mathrm{RM}\,\lambda^2$, where $\Delta\chi = \chi_\mathrm{obs} - \chi_0$, and χ_obs and χ_0 are the observed and intrinsic polarization angle, respectively. RM is the Faraday rotation measure, indicating the amount of rotation in the polarization angle in units of $\mathrm{rad\,m^{-2}}$. Based on this expression, one can calculate the RM using the following the equation, $\mathrm{RM} = (\chi_1 - \chi_2)/({\lambda_1}^2 - {\lambda_2}^2)$, where χ_1 and χ_2 are the observed polarization angles at wavelengths λ_1 and λ_2, respectively. For a cosmological source at redshift z, RM is defined as:

$$\mathrm{RM} = \frac{e^3}{2\pi {m_\mathrm{e}}^2 c^4} \frac{1}{(1+z)^2} \int n_\mathrm{e}(l)\, B_\parallel(l)\, dl, \qquad (1)$$

where m_e and e are the mass and charge of an electron, c is the speed of light, n_e is the electron number density of a Faraday screening medium, $B_\parallel$ is the magnetic field strength along the line-of-sight, and l is the path length through the medium where the Faraday rotation takes place.

[1] This might be related to B19 defined in Weaver et al. (2022).

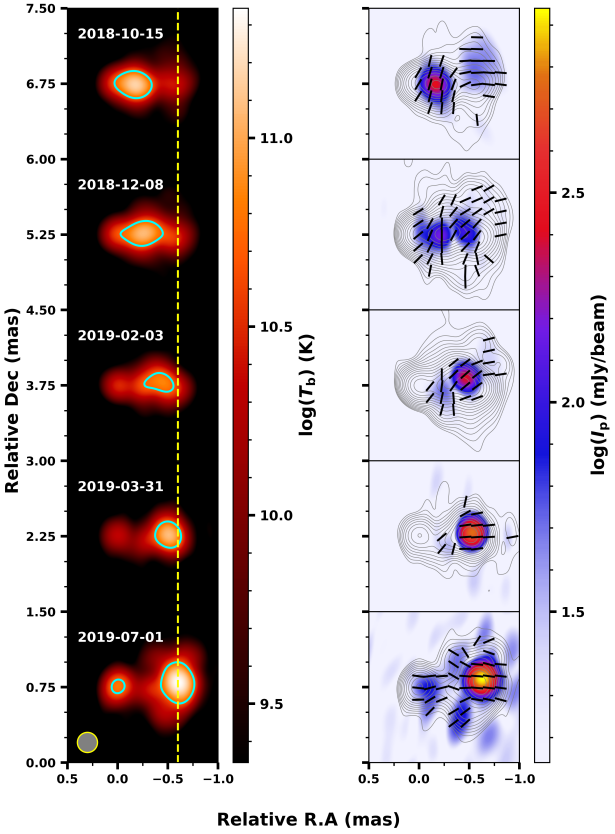

Fig. 2. Left: brightness temperature in the source-rest frame. The yellow-dashed line indicates the location of Region C ($\sim$ 0.6 mas from the core). The cyan contours show where $T_{\rm b} = 5 \times 10^{10}$ K (equipartition condition, Readhead, 1994). Right: polarized intensity maps. The black bars show the polarization angle (Jeong et al., in prep.).

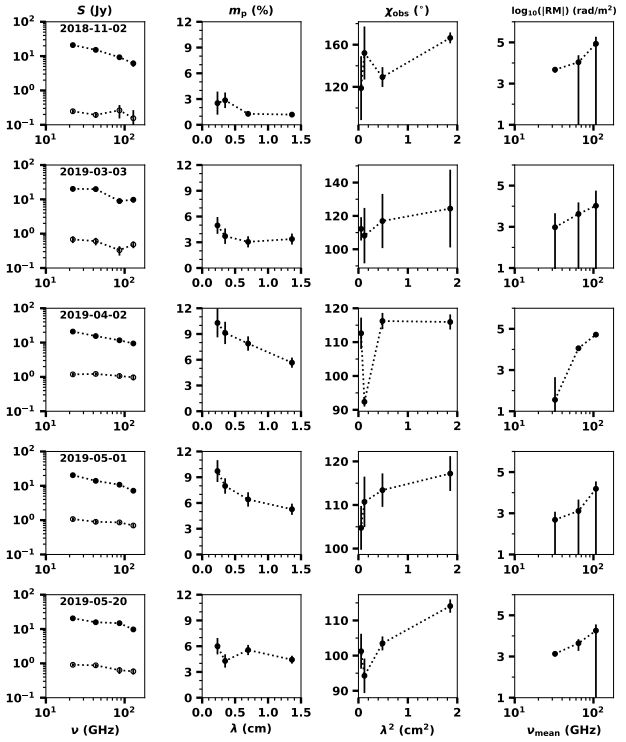

Fig. 3. From left to right panels, each shows total and polarized flux densities (filled and open circles, respectively), polarization degree, observed polarization angle, and log-absolute Faraday rotation measure near PF (Jeong et al., in prep.).

The blazar 3C 454.3 ($z = 0.859$) has been extensively investigated in multi-wavelength high-resolution polarization studies. In very long baseline interferometry (VLBI) observations at 15 GHz, the source was resolved with a widely extended jet structure beyond $\sim$10 milli-arcsecond (mas) from the central engine, ejecting toward the northwest side (Lister et al., 2018, 2021; Pushkarev et al., 2023). At 43 GHz, two prominent regions have been identified over a decade: the core and a quasi-stationary component (0.45–0.70 mas away from the core, hereafter, Region C, Jorstad et al., 2017; Weaver et al., 2022). Typically, Region C exhibits a higher polarization degree than that of the core with a stable polarization angle aligned to $\sim$ 90° (an east-west direction, Kemball et al., 1996; Jorstad et al., 2005, 2013; Traianou et al., 2024). Based on its observed properties (re-brightening, angular size decrease, and spatial stationariness), Region C was suggested as a recollimation shock (Gómez et al., 1999; Jeong et al., 2023). For a downstream region, Zamaninasab et al. (2013) found a large-scale helical magnetic field structure in 3C 454.3 by comparing the predictions of the helical jet model and observed polarimetric properties across the jet, using the multi-frequency Very Long Baseline Array (VLBA[2]) observations.

In this study, we investigate the decadal polarimetric characteristics of the source using the simultaneous multi-frequency (22 to 129 GHz) single-dish (SD) observations from the Korean VLBI Network (KVN[3]). We also employed the data from the 43-GHz VLBA, managed by the Boston University (BU[4]) group. The obtained VLBA data were used to compare with the KVN data at 43 GHz and to resolve the source structure. The data sets used in this study have a time range of 2011–2022, and several γ-ray activities were reported in this period (Buson, 2014; Jorstad et al., 2015; Ojha, 2016; Panebianco et al., 2022). The observations will be described in Section 2. The results and conclusions of this work will be presented in Secion 3.

Figure 3 shows the measurements from the KVN SD around PF. We found chromatic $m_{\rm p}$ in April 2019, near the peak of PF. To understand the origin of PF, we consider three cases: collision of a moving knot with external medium, magnetic reconnection, and shock–shock interac-

[2] https://science.nrao.edu/facilities/vlba
[3] https://radio.kasi.re.kr/kvn/main.php
[4] https://www.bu.edu/blazars/BEAM-ME.html

tion. The first case is less likely given the de-projected distance of Region C ($\sim$ 200 pc) and of the broad-line region of 3C 454.3 ($\sim$ 0.2 pc, Bonnoli et al., 2011; Costamante et al., 2018) and unstable Faraday RM. The second case[5] is difficult to explain the concurrent increase in S_I and S_p given particle-in-cell simulations (e.g., Zhang et al., 2020). The observed chromatic m_p and parallel χ_obs with jet direction can be explained through a shock–shock interaction in Region C (e.g., Marscher, 2014; Tavecchio et al., 2018, 2020; Liodakis et al., 2022).

Given the narrow viewing angle (θ_v) of 3C 454.3 ($\theta_\mathrm{v,mean} = 1.^\circ4 \pm 0.^\circ4$, Weaver et al., 2022), change in θ_v can attribute the PF via a strong Doppler boosting effect. If the jet is bent toward us in Region C, the expected increasing factor of brightness would be 1.28 ± 0.16, while the observed factor in T_b (Figure 2) is larger than 3.5. This implies an additional source-intrinsic process, such as particle acceleration in Region C. Therefore, among the three scenarios presented in this study, we suggest a shock–shock interaction in Region C, with possible additional particle acceleration, is most likely the origin of PF (Jeong et al., in prep.).

Acknowledgements. The KVN is a facility operated by the KASI (Korea Astronomy and Space Science Institute). The KVN observations and correlations are supported through high-speed network connections among the KVN sites provided by the KREONET (Korea Research Environment Open NETwork), which is managed and operated by KISTI (Korea Institute of Science and Technology Information). This work was supported by the National Research Foundation of Korea (NRF) grant funded by the Korea government (MIST) (2020R1A2C2009003). We also acknowledge financial support from the National Research Foundation of Korea (NRF) grant 2022R1F1A1075115. This study makes use of VLBA data from the VLBA-BU Blazar Monitoring Program (BEAM-ME and VLBA-BU-BLAZAR; http://www.bu.edu/blazars/BEAM-ME.html), funded by NASA through the Fermi Guest Investigator Program. The VLBA is an instrument of the National Radio Astronomy Observatory. The National Radio Astronomy Observatory is a facility of the National Science Foundation operated by Associated Universities, Inc. This work made use of Astropy:[6] a community-developed core Python package and an ecosystem of tools and resources for astronomy (Astropy Collaboration et al., 2013, 2018, 2022).

References

Astropy Collaboration, Robitaille, T. P., Tollerud, E. J., et al. 2013, A&A, 558, A33
Astropy Collaboration, Price-Whelan, A. M., Sipőcz, B. M., et al. 2018, AJ, 156, 123
Astropy Collaboration, Price-Whelan, A. M., Lim, P. L., et al. 2022, ApJ, 935, 167
Bonnoli, G., Ghisellini, G., Foschini, L., et al. 2011, MNRAS, 410, 368
Burn, B. J. 1966, MNRAS, 133, 67
Buson, S. 2014, The Astronomer's Telegram, 6236
Clark, B. G. 1980, A&A, 89, 377
Cornwell, T., Braun, R., & Briggs, D. S. 1999, Synthesis Imaging in Radio Astronomy II, 180, 151
Costamante, L., Cutini, S., Tosti, G., et al. 2018, MNRAS, 477, 4749
Gómez, J.-L., Marscher, A. P., & Alberdi, A. 1999, ApJ, 522, 74
Högbom, J. A. 1974, A&AS, 15, 417
Jeong, H.-W., Lee, S.-S., Cheong, W. Y., et al. 2023, MNRAS, 523, 5703
Jorstad, S. G., Marscher, A. P., Lister, M. L., et al. 2005, AJ, 130, 1418
Jorstad, S. G., Marscher, A. P., Stevens, J. A., et al. 2007, AJ, 134, 799
Jorstad, S. G., Marscher, A. P., Smith, P. S., et al. 2013, ApJ, 773, 147
Jorstad, S., Larionov, V., Mokrushina, A., et al. 2015, The Astronomer's Telegram, 7942
Jorstad, S. G., Marscher, A. P., Morozova, D. A., et al. 2017, ApJ, 846, 98
Kam, M., Trippe, S., Byun, D.-Y., et al. 2023, Journal of Korean Astronomical Society, 56, 1
Kang, S., Lee, S.-S., & Byun, D.-Y. 2015, Journal of Korean Astronomical Society, 48, 257
Kemball, A. J., Diamond, P. J., & Pauliny-Toth, I. I. K. 1996, ApJ, 464, L55
Liodakis, I., Marscher, A. P., Agudo, I., et al. 2022, Nature, 611, 677
Lister, M. L., Aller, M. F., Aller, H. D., et al. 2018, ApJS, 234, 12
Lister, M. L., Homan, D. C., Kellermann, K. I., et al. 2021, ApJ, 923, 30
Marscher, A. P. 2014, ApJ, 780, 87
Ojha, R. 2016, The Astronomer's Telegram, 9190
Panebianco, G., Bulgarelli, A., Pittori, C., et al. 2022, The Astronomer's Telegram, 15782
Park, J., Kam, M., Trippe, S., et al. 2018, ApJ, 860, 112
Pushkarev, A. B., Aller, H. D., Aller, M. F., et al. 2023, MNRAS, 520, 6053
Readhead, A. C. S. 1994, ApJ, 426, 51
Shepherd, M. C. 1997, Astronomical Data Analysis Software and Systems VI, 125, 77
Sokoloff, D. D., Bykov, A. A., Shukurov, A., et al. 1998, MNRAS, 299, 189
Tavecchio, F., Landoni, M., Sironi, L., et al. 2018, MNRAS, 480, 2872
Tavecchio, F., Landoni, M., Sironi, L., et al. 2020, MNRAS, 498, 599
Traianou, E., Krichbaum, T. P., Gómez, J. L., et al. 2024, A&A, 682, A154
Weaver, Z. R., Jorstad, S. G., Marscher, A. P., et al. 2022, ApJS, 260, 12
Zamaninasab, M., Savolainen, T., Clausen-Brown, E., et al. 2013, MNRAS, 436, 3341
Zhang, H., Li, X., Giannios, D., et al. 2020, ApJ, 901, 149

[5] For a magnetic reconnection, two plasmoids interact with each other, leading to the disordering of magnetic field lines, and thus weak polarized emission.

[6] http://www.astropy.org